Supplementary Materials for

Plant-derived exosome-like nanovesicles improve testicular injury by alleviating cell cycle arrest in Sertoli cells

Yuling Xiao, Xingzi Hou, Chenlong Wei, Meng Ding, Wangxiao Tan, Pengfei Tu, Xiao Zhang*, and Yong Jiang*

State Key Laboratory of Natural and Biomimetic Drugs, School of Pharmaceutical Sciences, Peking University, Beijing 100191, China

*Corresponding authors.

E-mail addresses: yongjiang@bjmu.edu.cn (Yong Jiang), xiao_zhang@bjmu.edu.cn (Xiao Zhang).

The PDF file includes:

Supplementary Figs. 1 to 9

Supplementary Tables 1 to 3

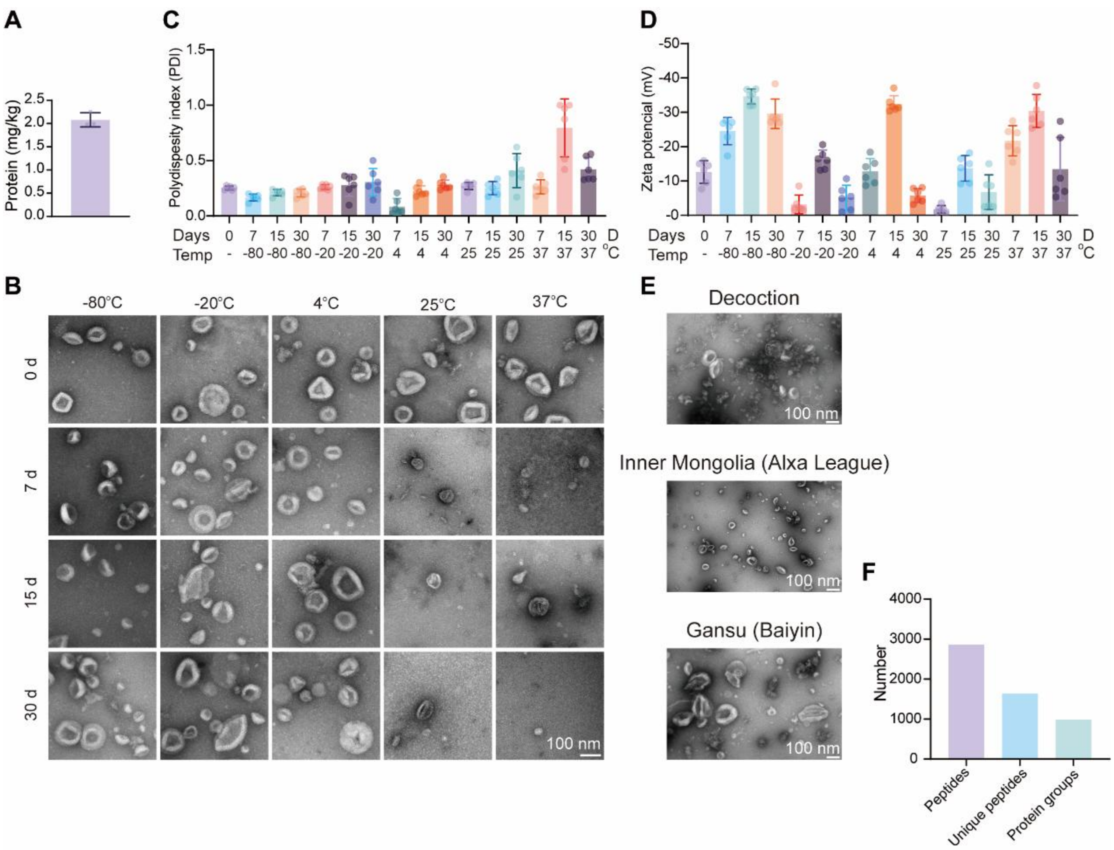

Supplementary Fig. 1 Characterization of CDELNs. **A** Quantification of CDELNs yield from *Cistanche deserticola* by protein concentration determined with the BCA assays ($n = 3$). **B** Representative TEM images of CDELNs stored at different temperatures (–80, –20, 4, 25, and 37°C) for varying durations (0, 7, 15, and 30 days). **C, D** polydispersity index (**C**) and Zeta potential (**D**) of CDELNs under different storage conditions as determined by dynamic light scattering (DLS). **E** TEM images of CDELNs derived from water decoction and different geographical sources. **F** Statistical analysis of the number of identified peptides and proteins in the proteomic profiling of CDELNs. Data are presented as the means ± SDs.

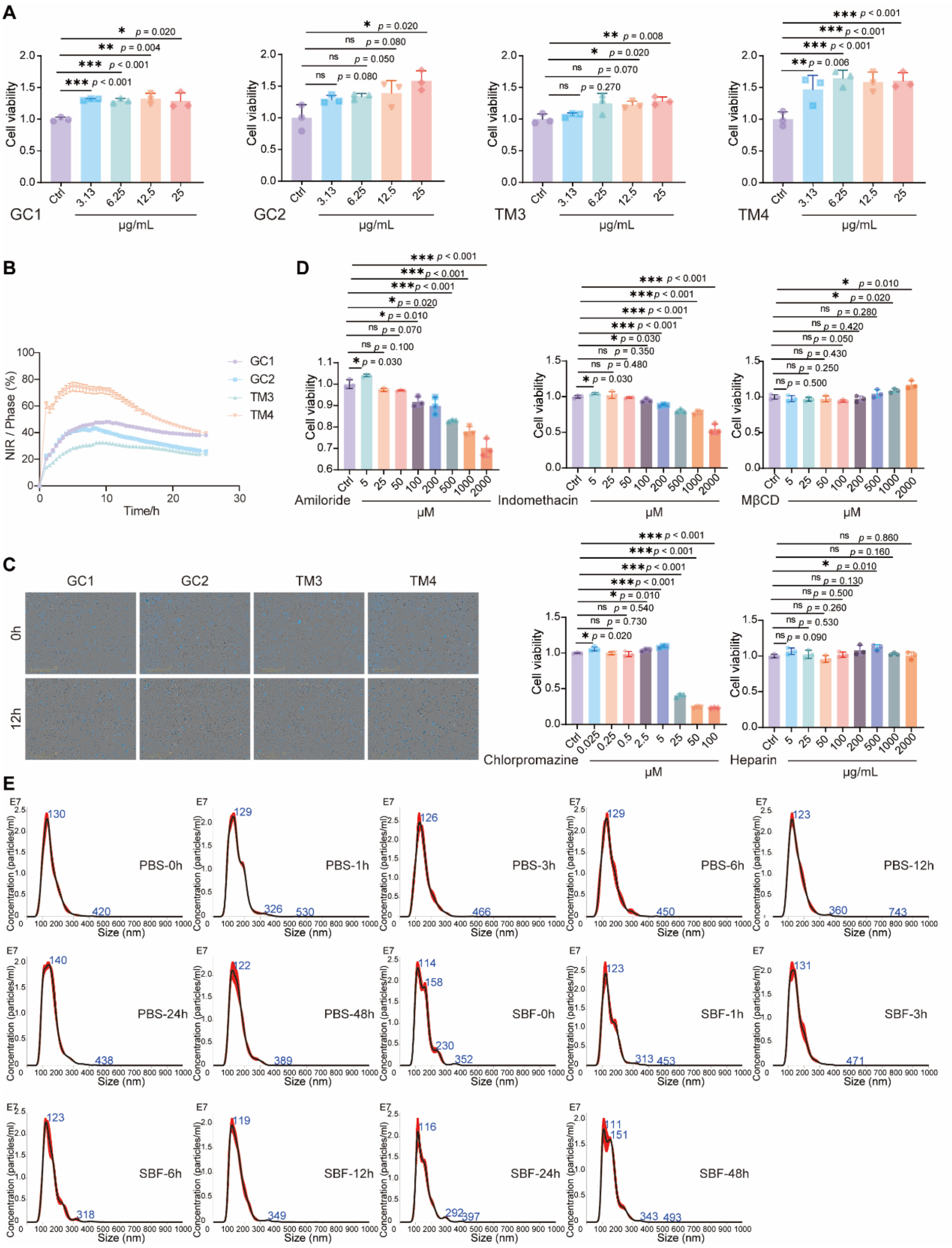

Supplementary Fig. 2 ***In vitro*** **cytotoxicity, cellular uptake and stability analysis of CDELNs. A** Cytotoxicity of CDELNs on four testicular cell lines (GC1, GC2, TM3, TM4) by MTT assay ($n = 3$). **B** Cellular uptake of DiD-CDELNs in four testicular cell lines by long time-lapse imaging. **C** Bright-field images of four testicular cell lines treated with DiD-CDELNs. **D** Cytotoxicity of various endocytic inhibitors (amiloride, indomethacin, MβCD, chlorpromazine, heparin) on TM4 cells by MTT assay ($n = 3$). **E** Size distribution of CDELNs incubated in PBS and simulated body fluid (SBF) for different durations (0, 1, 3, 6, 12, 24, and 48 h) using NTA. Data are presented as the means ± SDs.

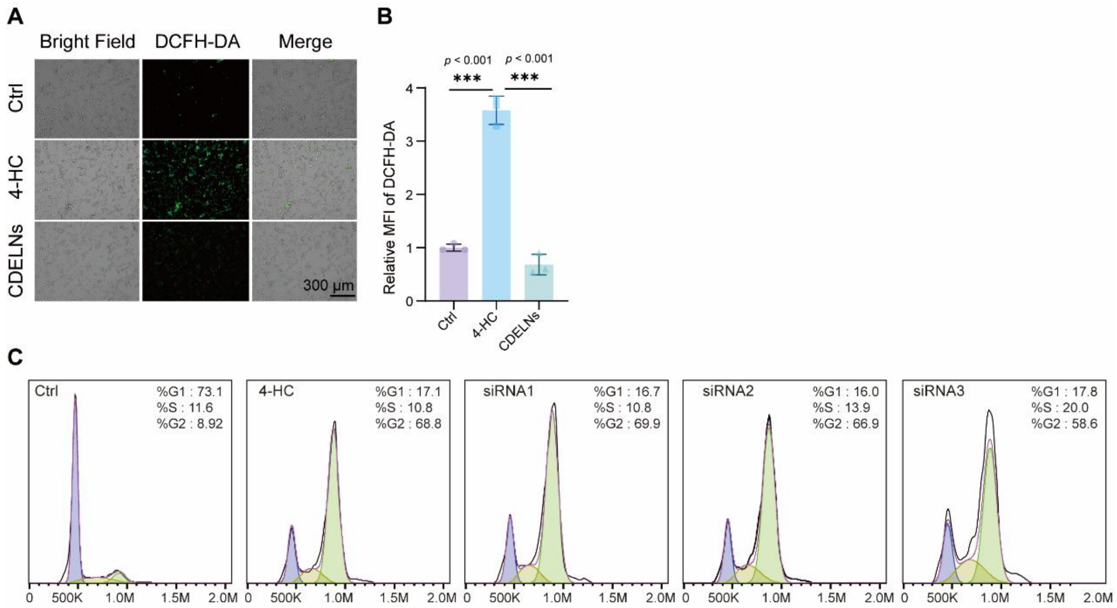

Supplementary Fig. 3 CDELNs alleviated 4-HC-induced TM4 cell injury *in vitro*. A Representative fluorescence images of reactive oxygen species (ROS) in TM4 cells treated with 4 μM 4-HC upon CDELNs interventions. **B** Quantitative analysis of mean fluorescence intensity of ROS in (**A**) (n = 3). **C** Cell cycle analysis of TM4 cells treated with 4 μM 4-HC after transfection with three independent p21 siRNAs by flow cytometric analysis. Data are presented as the means ± SDs.

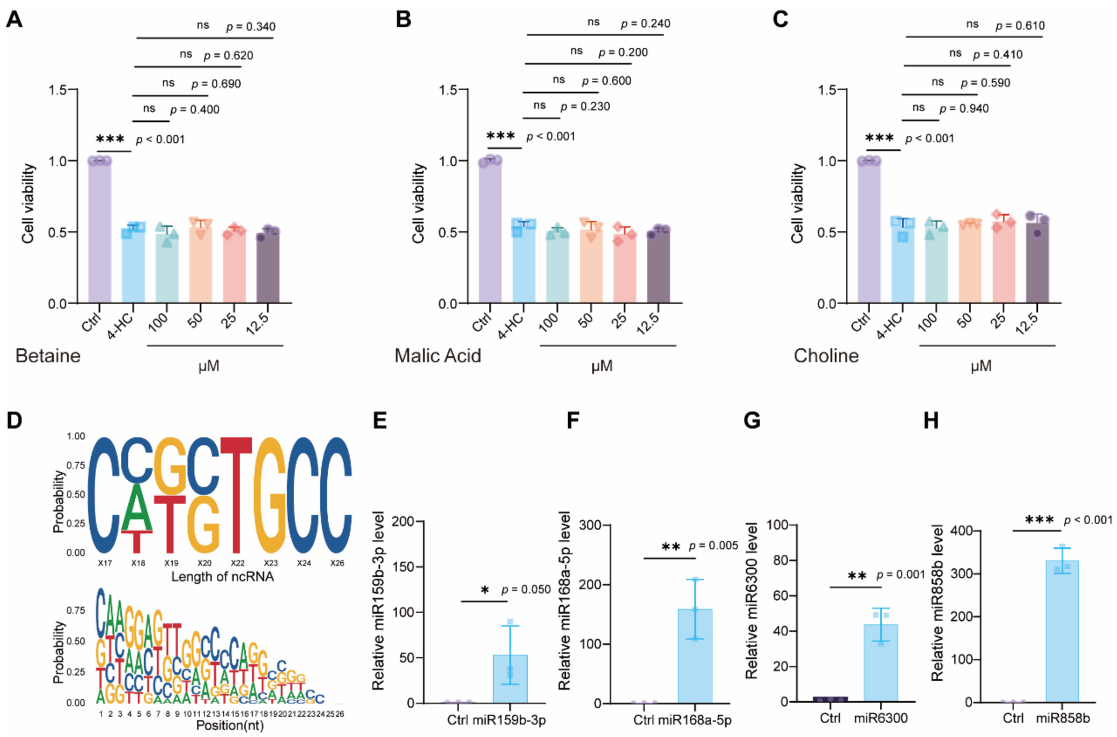

Supplementary Fig. 4 Identification of bioactive components in CDELNs. A−C Cell viability of TM4 cells treated with 4 μM 4-HC upon betaine (**A**), malate (**B**), and choline (**C**) interventions by MTT assay (*n* = 3). **D** First nucleotide bias of known miRNAs (17–26 nt) in CDELNs (Top). miRNA nucleotide bias at each position (Bottom). **E−H** qRT-PCR analysis of miR159b-3p (**E**), miR168a-5p (**F**), miR6300 (**G**), and miR858b (**H**) in TM4 cells transfected with their mimics (*n* = 3). Data are presented as the means ± SDs.

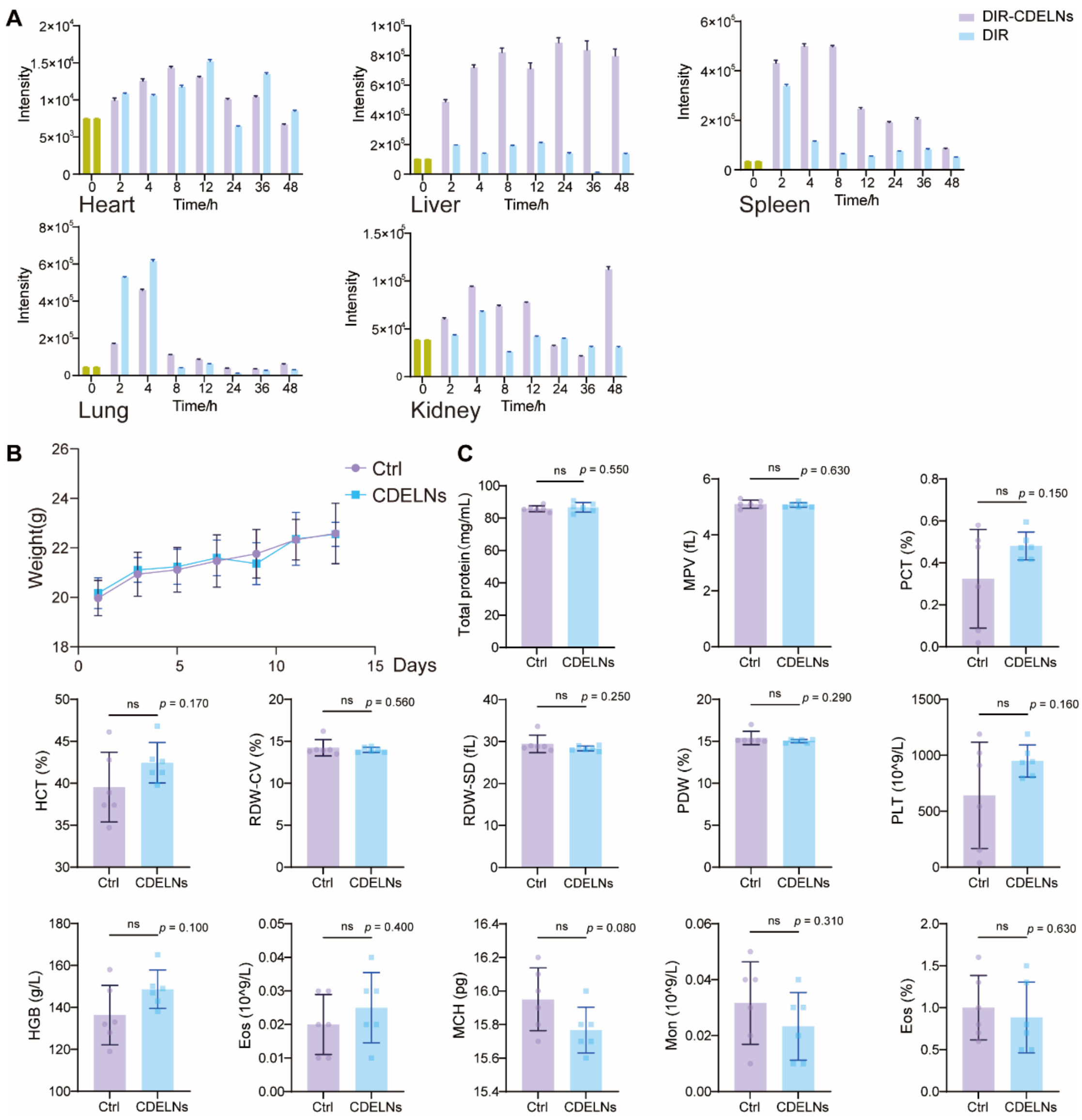

Supplementary Fig. 5 Biosafety assessment of CDELNs *in vivo*. A Fluorescence intensity of DiR or DiR-CDELNs in mouse heart, liver, spleen, lung, kidney. Data are presented as the means ± SEMs. n = 10 technical replicates. **B** Body weight of mice measured over 14 days following intraperitoneal administration of CDELNs (n = 6). **C** Blood routine test after 14 days of intraperitoneal injection of CDELNs, including Total protein, Mean Platelet Volume (MPV), Plateletcrit (PCT), Hematocrit (HCT), Red Cell Distribution Width-Coefficient of Variation (RDW-CV), Red Cell Distribution Width-Standard Deviation (RDW-SD), Platelet Distribution Width (PDW), Platelet (PLT), Hemoglobin (HGB), Eosinophil (Eos), Mean Corpuscular Hemoglobin (MCH), and Monocyte (Mon) (n = 6). Data are presented as the means ± SDs.

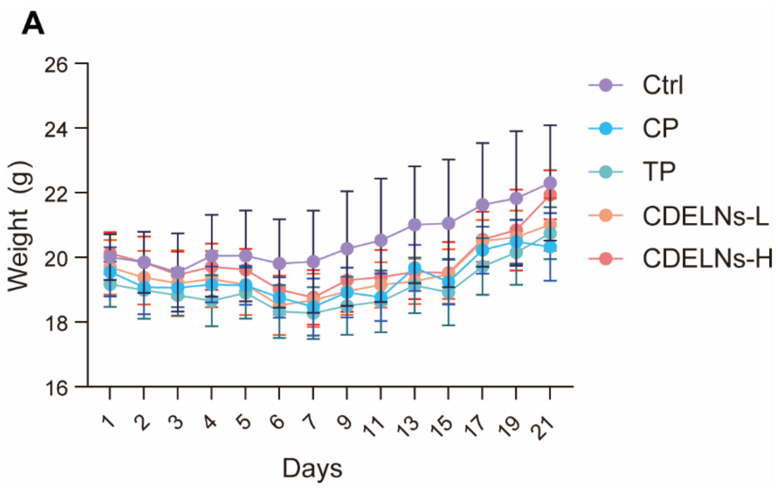

Supplementary Fig. 6 CDELNs alleviated cyclophosphamide (CP)-induced male reproductive injury. A Body weight of mice throughout the experimental period (n = 6). Data are presented as the means ± SDs.

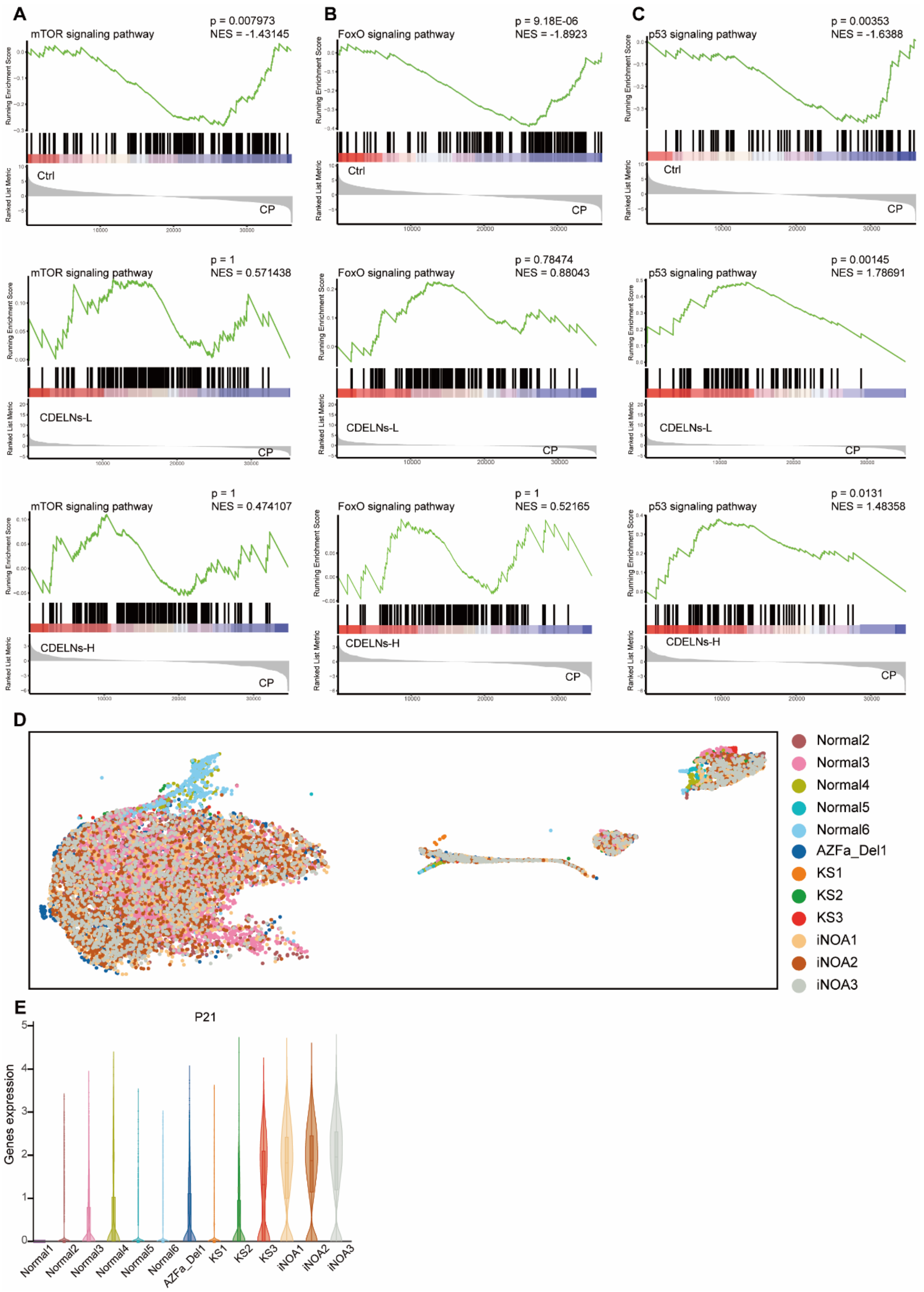

Supplementary Fig. 7 Bioinformatics analyses of multi-omic data about male reproductive injury. **A−C** Signature enrichment plots from GSEA analysis using signature gene sets of mTOR(**A**), FoxO (**B**), and p53 (**C**) signaling pathway in CP-treated mice upon CDELNs interventions. **D** Analysis of normal Sertoli cells merged with iNOA, AZFa_Del, and KS Sertoli cells, in a UMAP plot with cells colored by sample type (*n* (normal) = 5, *n* (iNOA) = 3, *n* (AZFa_Del) = 1, *n* (KS) = 3). **E** Violin plot of the expression levels of P21 in normal and NOA testes.

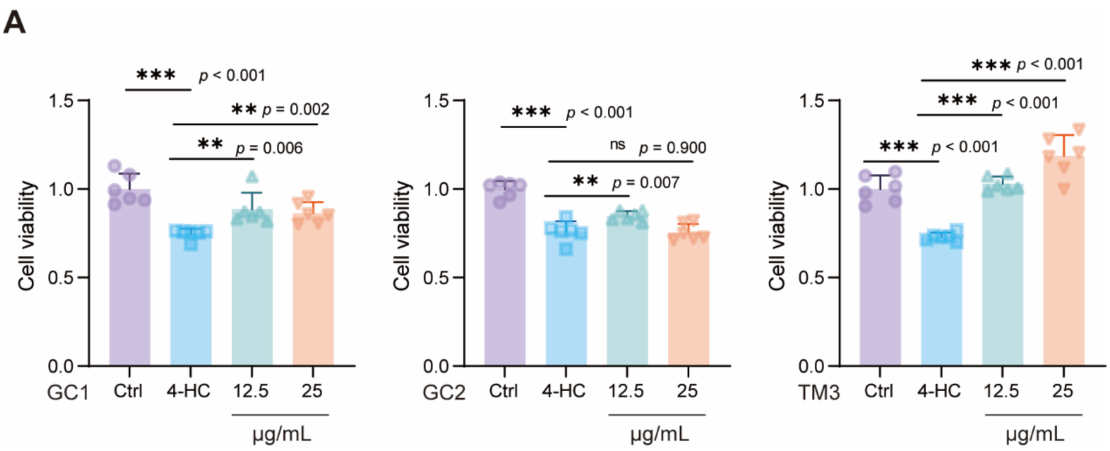

Supplementary Fig. 8 CDELNs alleviated 4-HC-induced GC1/GC2/TM3 cell injury *in vitro*. A CDELNs increased cell viability against 4-HC induced injury in GC1, GC2, and TM3 cells (n = 6). Data are presented as the means ± SDs

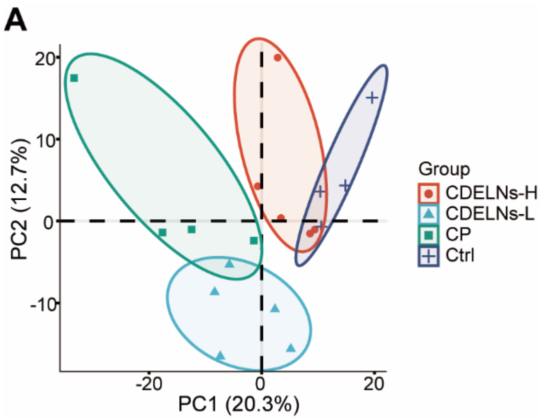

Supplementary Fig. 9 CDELNs intervention reshapes the metabolic profile of CP-injured testes. A Principal component analysis (PCA) of the serum metabolome from CP-treated mice upon CDELNs interventions ($n \geqslant 4$).

Supplementary Table 1 Primer sequences used for qRT-PCR

Primers	Forward (5'-3')	Reverse (5'-3')
P21	CCTTGTCGCTGTCTTGCACTCTG	GCTGGTCTGCCTCCGTTTTCG
β-actin	AGAGGGAAATCGTGCGTGAC	CAATAGTGATGACCTGGCCGT
rgl-miR7972	CGCTTGTCAGGCTTGTTATTCTCC	AGTGCAGGGTCCGAGGTATT
ptc-miR6478	CCGACCTTAGCTCAGTTGGTG	AGTGCAGGGTCCGAGGTATT
ptc-miR399e	ATTCGCCAAAGGAGAGTTGCCCT	AGTGCAGGGTCCGAGGTATT
ppt-miR894	CGTTTCACGTCGGGTTCACC	AGTGCAGGGTCCGAGGTATT
pab-miR858a	CTTCGTTGTCTGTTCGACCCTG	AGTGCAGGGTCCGAGGTATT
osa-miR5072	ATTATCGATTCCCCAGCGGAGTC	AGTGCAGGGTCCGAGGTATT
osa-miR1863b	CGCAGCTCTGATACCATGTTAACTGTT	AGTGCAGGGTCCGAGGTATT
osa-miR159f	CGCTTGGATTGAAGGGAGCTCTA	AGTGCAGGGTCCGAGGTATT
mdm-miR858	CTTCGTTGTCTGTTCGACCTGA	AGTGCAGGGTCCGAGGTATT
mdm-miR1511	CCGACCTAGCTCTGATACCATGAA	AGTGCAGGGTCCGAGGTATT
lus-miR159b	CGCTTTGGATTGAAGGGAGCTCTC	AGTGCAGGGTCCGAGGTATT
lja-miR168-5p	ATATTATCGCTTGGTGCAGGTCGG	AGTGCAGGGTCCGAGGTATT
htu-miR171a	GCTGATTGAGCCGTGCCAATAT	AGTGCAGGGTCCGAGGTATT
gma-miR6300	GCGCGGTCGTTGTAGTATAGTGG	AGTGCAGGGTCCGAGGTATT
fve-miR159a-5p	CCGGAGCTCCTTGAAGTCCAATAG	AGTGCAGGGTCCGAGGTATT
fve-miR1511	GCGACCTAGCTCTGATACCATGTG	AGTGCAGGGTCCGAGGTATT
far-miR159	CGTTTGGATTGAAGGGAGCTCTG	AGTGCAGGGTCCGAGGTATT
csi-miR171a	CGTTGAGCCGTGCCAATATCAC	AGTGCAGGGTCCGAGGTATT
cme-miR319c	TTGGACTGAAGGGAGCTCCT	AGTGCAGGGTCCGAGGTATT
cme-miR168	ATTATCGCTTGGTGCAGGTCGG	AGTGCAGGGTCCGAGGTATT
ath-miR858b	CGCTTCGTTGTCTGTTCGACCTTG	AGTGCAGGGTCCGAGGTATT
ath-miR8175	TATTATTGATCCCCGGCAACGGC	AGTGCAGGGTCCGAGGTATT
aqc-miR166a	TCGGACCAGGCTTCATTCCTC	AGTGCAGGGTCCGAGGTATT
aly-miR858-5p	GGCTTTCGTTGTCTGTTCGACCTT	AGTGCAGGGTCCGAGGTATT
aly-miR396b-5p	CCGCTTCCACAGCTTTCTTGAACTT	AGTGCAGGGTCCGAGGTATT
aly-miR171b-3p	TTGAGCCGTGCCAATATCACG	AGTGCAGGGTCCGAGGTATT
aly-miR168a-5p	AATATCGCTTGGTGCAGGTCGG	AGTGCAGGGTCCGAGGTATT
aly-miR168a-3p	CCCGCCTTGCATCAACTGAAT	AGTGCAGGGTCCGAGGTATT
aly-miR159b-3p	CCGTTTGGATTGAAGGGAGCTCTT	AGTGCAGGGTCCGAGGTATT
aly-miR157d-3p	GCGGCTCTCTATGCTTCTGTCATC	AGTGCAGGGTCCGAGGTATT
ahy-miR159	CGCTTTGGATTGAAGGGAGCTCTA	AGTGCAGGGTCCGAGGTATT
aau-miR396	CGCTTCCACAGCTTTCTTGAACTG	AGTGCAGGGTCCGAGGTATT
U6	CGCTTCCACAGCTTTCTTGAACTG	AACGCTTCACGAATTTGCGT

Supplementary Table 2 Sequence of miRNA mimics and miR159b-3p inhibitor/probe

Name	Forward (5'-3')	Reverse (5'-3')
NC mimic	UUGUACUACACAAAAGUACUG	GUACUUUUGUGUAGUACAAUU
miR858b mimic	UUCGUUGUCUGUUCGACCUUG	AGGUCGAACAGACAACGAAUU
miR6300 mimic	GUCGUUGUAGUAUAGUGG	ACUAUACUACAACGACUU
miR168a-5p mimic	UCGCUUGGUGCAGGUCGGGAA	CCCGACCUGCACCAAGCGAUU
miR159b-3p mimic	UUUGGAUUGAAGGGAGCUCUU	GAGCUCCCUUCAAUCCAAAUU
miR159b-3p inhibitor	AAGAGCUCCCUUCAAUCCAAA	
Cy3-labeled miR159b-3p probe	AAGAGCTCCCTTCAATCCAAA	

Supplementary Table 3 Sequence of P21 siRNAs

siRNA	Forward (5’-3’)	Reverse (5’-3’)
siRNA 1	CUGAAUAGCACUUUGGAAATT	UUUCCAAAGUGCUAUUCAGTT
siRNA 2	GAGCAUGAAUGGAGACAGATT	UCUGUCUCCAUUCAUGCUCTT
siRNA 3	GGUCCUUGGUGGUGAGACATT	UGUCUCACCACCAAGGACCTT